Formylpeptide receptor 1 expression in human glioblastoma

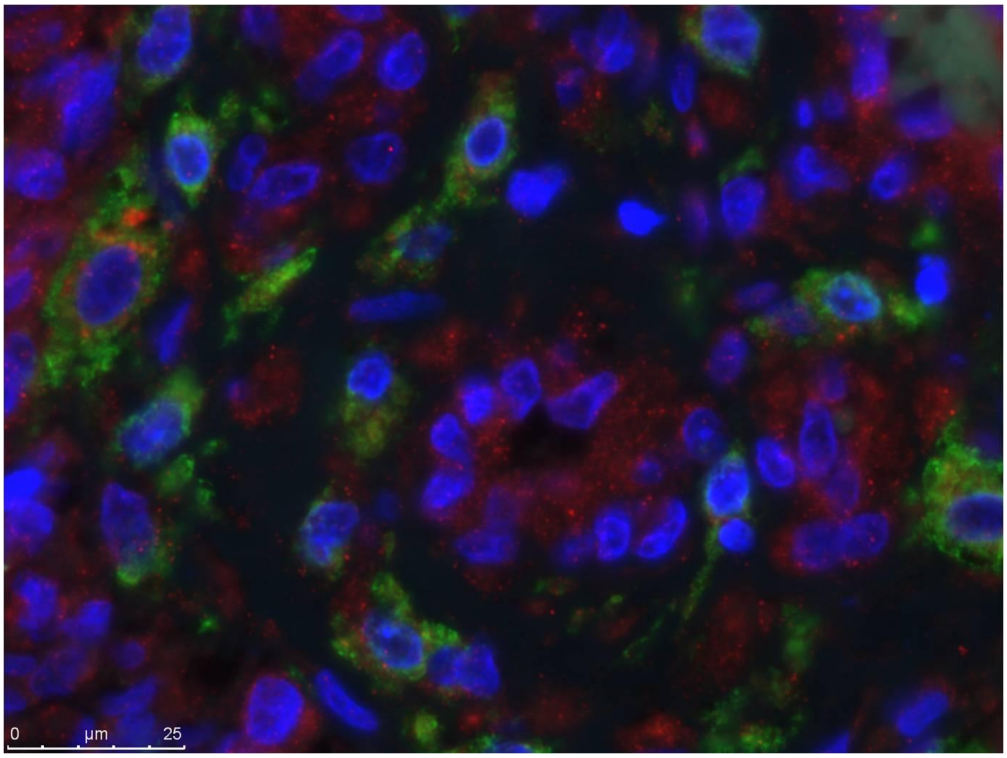

Author: Yannick van Sleen (s1777793)

Supervisors: Dr. W.F.A. den Dunnen, Dr U.L.M Eisel and PhD. J.C. Boer

Institute: University Medical Centre Groningen (UMCG)

Departments: Pathology and Medical Oncology

Period: February 2013 – August 2013

umcg

rijksuniversiteit groningen

Abstract

Introduction: Glioblastoma (GBM) is the most malignant type of brain tumors in adults. Activation of the formylpeptide receptor 1 (FPR1) in phagocytic leukocytes leads to chemotaxis towards a bacterial infection and phagocytosis. FPR1 expression is also found in many human GBMs, where its activation promotes angiogenesis, proliferation and tumor cell migration. The main goal of this study was to investigate why the majority of the recently cultured GBM cell lines (the GG cell lines) are lacking FPR1 expression. Another goal of this study was to investigate the effect of the FPR1 antagonist Chemotaxis inhibitory protein of *S. aureus* (CHIPS) on the only FPR1 positive cell line GG5 *in vivo*. We also investigated whether variation in FPR1 expression correlates with the molecular GBM subtypes (proneural, mesenchymal, classic and neural).

Material and methods: A staining for FPR1 was performed on snap-frozen human GBMs (n=36) and formalin fixed, paraffin embedded (FFPE) human GBMs (n=128) on a tissue micro-array (TMA). FPR1 expression was quantified on snap frozen tissues by evaluating the percentage of positive cells and the antigenic load and for the FFPE with an intensity scale from 0-3. The FPR1 expression on frozen tissues was matched with survival data and the FPR1 expression on FFPE tissues with their molecular GBM subtype. A fluorescent doublestaining of FPR1 CD68, CD163 and GFAP was performed on human FFPE GBM tissues. Five GG cell lines were implanted in mouse brains and the FPR1 expression of the resulting tumor was evaluated. CHIPS(n=6) and PBS (n=3) treated GG5 xenografts were stained for: Angiopoeitin-1, Angiopoeitin-2, Tie-2, Ki67, cleaved caspase-3 and FPR1 on snap frozen or FFPE tissue. A GLUT-1 staining helped distinguishing normoxic from hypoxic regions, as the expression of each marker was separately evaluated for the normoxic and hypoxic zone.

Results: FPR1 expression is found in all human GBM tissues. The average percentage of FPR1 positive cells in snap frozen GBMs was 35%, while the majority of the FFPE GBMs showed FPR1 expression in every cell. A negative trend was found between the percentage of FPR1 positive cells in snap frozen GBMs and patient survival. No significant differences were found in the FPR1 intensity score for the four molecular GBM subtypes. FPR1 is found to co-express with CD68, CD163 and GFAP in all patients specimens. All five tumors resulting from implanted GG cell lines in mouse brains are FPR1 positive. No differences were found in angiogenesis, proliferation and apoptosis markers between tumors of CHIPS treated and untreated animals.

Conclusion: This study shows widespread FPR1 expression in all human GBMs, but its expression does not correlate with any molecular subtype or with patient survival. Microenvironmental factors may be necessary to maintain FPR1 expression in GBM cells. CHIPS treatment of GG5 xenografts did not show any effects on proliferation and apoptosis

Introduction

Glioblastoma multiforme

Gliomas are the most common of all primary brain tumors and can be divided into two main categories: astrocytic and oligodendric. Oligodendroglioma arise from oligodendrocytes and are quite slowly growing neoplasms with median survival times of several years (Ohgaki and Kleihues, 2005). Astrocytomas are the most common type of glial tumors; they are malignant neoplasms that arise from astrocytes. Astrocytomas are known to be histologically and genetically heterogeneous and thus require different therapeutical approaches (DeAngelis, 2001). These tumors are histologically classified according to the World Health Organization (WHO) based on their aggressiveness. This classification ranges from slowly growing low-grade tumors (grade I and II) to rapidly growing high-grade tumors (grade III and IV). Grade IV astrocytoma is generally referred to as glioblastoma multiforme (GBM). (Louis et al., 2007).

Patients with grade II astrocytoma have a median survival after diagnosis of approximately 7 years (Louis et al., 2007), whereas the majority of GBM patients have a median survival of only 12-15 months (Wen and Kesari, 2008). GBM is the most common type of malignant primary brain tumors and it accounts for 60-75% of astrocytic tumors. GBM especially affects adults, with a peak incidence in the sixth or seventh decade (DeAngelis, 2001).

The incidence of high grade astrocytomas is lower than many other types of cancer, 3-4 new cases per 100.000 population per year (DeAngelis, 2001), but due to its high mortality it is still ranked high in the leading causes of cancer-related deaths (Boring et al., 1994). The overall incidence of GBM has remained stable in the Netherlands between 1989 and 2003 (Houben et al., 2006).

Primary glioblastomas are associated with a high rate of overexpression or mutation of the epidermal growth factor receptor, p16 deletions, and mutations in the gene for phosphatase and tensin homologues (PTEN) (Watanabe et al., 1996; Tohma et al., 1998). GBMs are mostly localized in the cerebral hemispheres and are differentiated from lower graded tumors by the presence of severe necrosis and hyperplastic blood vessels. (Chen et al., 2013) The level of necrosis in GBM is a strong predictor of poor prognosis, probably because at the time necrosis occurs, the tumor cells have reached a highly malignant state (Louis, 2006).

Distant metastasis of GBM is very uncommon, but local invasion of surrounding brain tissue is the hallmark of malignant gliomas. Tumor cells diffusely invade and permeate into the surrounding brain parenchyma and may even cross the midline to the contralateral brain (Wilson et al., 1992) (See fig 1). Migrating invasive tumor cells can be identified following myelinated fiber tracts, along basement membranes of blood vessels and within the perivascular spaces. Marginal region tumor cells are more migratory and more resistant to apoptosis compared to cells in the tumor core (Giese et al., 2003).

Molecular subtypes could recently be defined in which a major portion of the GBM population could be fit. The classic subtype is known for the highest level of chromosome 7 amplification, leading to EGFR upregulation. No p53 mutations are found for this subtype. The proneural subtype is correlated with mutations in p53, IDH1 and the PDGF receptor and mostly occurs in younger patients. The neural subtype is probably the rarest and is correlated with EGFR amplification and with neural markers. These tumors have the most in common with normal brain tissue. Finally, mesenchymal tumors rarely exhibit EGFR upregulation, but do show decreased NF1 expression. These tumors are defined by mesenchymal markers like CHI3L1 and MET. Difficulties arise in subtyping GBMs, as an important part of these tumors share characteristics with two or more GBM subtypes (Phillips et al., 2006; Verhaak et al., 2010).

Treatment of GBM consists of a combination of neurosurgery, radiotherapy and chemotherapy with Temazolomide (Stupp et al., 2009). This therapy increases overall survival with approximately 8-11 months (Van Meir et al., 2010). Extensive resection of surrounding brain tissue may enhance the effect of the combined therapy, although this is accompanied by loss of neurological function (Wang et al., 2013). Each molecular subtype requires different therapeutic approaches, which could be of importance in the treatment of the disease subtypes (Phillips et al., 2006; Verhaak et al., 2010). The invasive phenotype of GBM is a fundamental reason of recurrence after treatment and thus for treatment failure. To counteract the extensive infiltrative nature of GBM, the migration of tumor cells needs to be targeted.

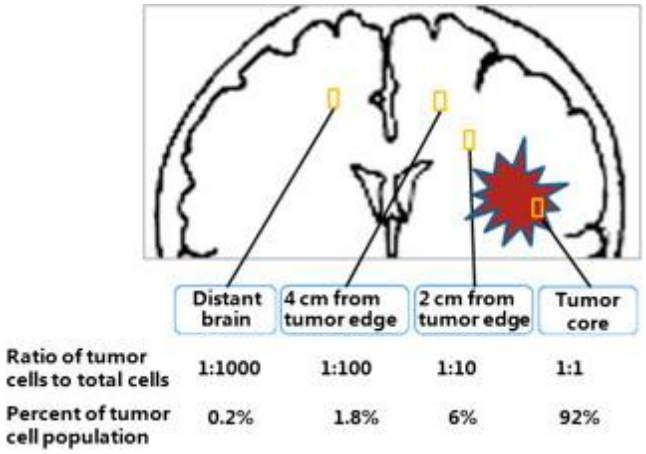

Fig 1: tumor cells in GBM are mainly located in the tumor core, but also outside the core many tumor cells are found, sometimes these cells even cross the midline to the contralateral brain.This local invasion of GBM tumor cells into the surrounding brain tissue is a major cause of recurrent tumors after treatment (Wang et al., 2013).

The original role of FPR1

Before the discovery of the formyl peptide receptor, it's most potent ligand was discovered: *N*-formyl-methionyl-leucyl-phenylalanine, or fMLF (Showell et al., 1976) The *E. coli*-derived formyl peptide fMLF is considered a 'classical' chemoattractant, just like the activated complement component 5 (C5a), leukotriene B4 (LTB4) and patelet-activating factor (PAF) (Murphey et al., 1994). Chemoattractants create a concentration gradient up to which phagocytic leukocytes can migrate to the site of infection after the leukocytes have left the blood circulation by diapedesis (Prossnitz and Ye, 1997). Phagocytic leukocytes, including neutrophils and macrophages, are recruited to the site of infection as an immediate innate response of the host against microbial infection. These leukocytes are responsible for phagocytosis of the microbes (Abbas et al., 2010).

The chemoattractants activate GPCRs on their target cells, the phagocytic leukocytes. The presence of a functional receptor for fMLF on leukocytes was expected, as *N*-formyl peptides could stimulate neutrophil chemotaxis and lysosomal enzyme release (Ye et al., 2009). The fMLF receptor binds FPR1 with the highest affinity, although many more agonists were found, including formyl peptides derived from ruptured mitochondria from necrotic cells (Ye et al., 2009; Rabiet et al., 2005). Later, receptors were found that shared significant sequence homology with FPR1. FPR2, discovered in 1992 by Ye et al. shares 68% of identical amino acids to FPR1 (Ye et al., 2009); FPR3 was also identified in 1992 (Murphey et al., 1992) and shares 58%

of identical amino acids to FPR1 (Ye et al., 2009). FPR1 is not only found in phagocytic leukocytes, but also in some cell types of non-hematopoietic origin including neurons, hepatocytes and lung epithelial cells (Becker et al., 1998).
When FPR1 binds with its agonist, a signal transduction pathway is initiated; this also involves release of cytoplasmic Ca^{2+}. This Ca^{2+} release leads to cell migration, phagocytosis and release of proinflammatory mediators. This is necessary for phagocytic leukocytes to clear invading bacteria (Huang et al., 2008; Partida-Sanchez et al., 2001). Other proteins involved in this cascade are PI3Kγ, NF-κB, ERK ½, Akt and MAPKs (Ye et al., 2009).
FPR1 knockout mice have defective chemotaxis of their neutrophils toward fMLF, were more susceptible to *L. monocytogenes* infection and showed an increased mortality rate (Gao et al., 1999). Chemotaxis inhibitory protein of *S. aureus* (CHIPS) is by far the most potent antagonist for FPR1 (pK_d of 7.46). This protein has also antagonistic activity for the C5a receptor. It binds directly on the receptor on the extracellular surface and thereby prevents the binding of natural agonists like fMLF. CHIPS is capable in preventing neutrophil responses to bacterial infection. Therefore the existence of this bacterial derived protein suggests a mechanism used by microbes to thwart host defenses (Haas et al., 2004; Postma et al., 2004).

FPR1 expression in glioblastoma multiforme

FPR1 expression in gliomas demonstrated was for the first time in 2000 by Le et al., who showed in an astrocytoma cell line (U87) that fMLF increases the secretion of proinflammatory IL-6 via the FPR1 receptor. FPR1 expressing tumor cells respond to fMLF by increased motility, proliferation, and angiogenesis and by transactivating the epidermal growth factor receptor (EGFR) (Zhou et al., 2005). EGFR has been found in high levels in human gliomas and is considered as one of the strongest growth-stimulating factors in tumors. EGFR activation by FPR1 is accounted for 40% of the biological activity of FPR1 in gliomas (Huang et al., 2008). Glioma clones expressing high levels of FPR1 show a more motile phenotype in vitro compared to those lacking FPR1. Only highly FPR1 expressing clones invaded surrounding connective tissue in mouse xenografts (Huang et al., 2010). FPR1 expression was found in the majority of glioblastomas (Zhou et al., 2005) but also in lower grade gliomas (Boer et al., 2013).
Glioblastomas are known for compressing surrounding brain tissue and for having large necrotic regions. Mitochondrial formyl peptides from ruptured cells in these regions are found to have affinity for FPR1 (analogously to fMLF) (Rabiet et al., 2005; Zhou et al., 2005). FPR1 expressing glioblastoma cell lines exhibit calcium flux upon stimulation with the mitochondrial peptides fMMYALF and fMLKLIV, showing that these peptides serve as a ligand for FPR1 (Boer et al., 2013). Because of the high level of necrosis in GBM, the relevance of targeting FPR1 may be higher than in lower graded astrocytomas (Louis et al., 2007). FPR1 may promote tumor growth and invasion of surrounding brain parenchyma in GBM mouse models and is therefore identified as a supporting factor in the malignancy of GBM (Huang et al., 2010; Zhou et al., 2005).
In vitro and in vivo experiments show that depletion of FPR1 by short interfering RNA (siRNA) resulted in substantially reduced tumorigenicity. This is demonstrated by an almost completely abolished fMLF-induced chemotaxis and reduced cell proliferation rate in FPR1-siRNA U87 cells. Mouse xenograft tumors formed out of FPR1-siRNA U87 cells had a reduced size compared to normal U87 tumors (Le et al., 2004; Zhou et al., 2005).

Because delivering siRNA to tumor cells remains challenging in the clinical practice, targeting FPR1 was accomplished by administering the antagonist CHIPS. In a previous study from Boer et al CHIPS was used to block binding of fMLF and mitochondrial peptides fMMYALF and fMLKLIV

on the FPR1 receptor in the astrocytoma cell line U87. Adding CHIPS indeed results in a dose-dependent inhibition of fMLF, fMMYALF and fMLKLIV induced calcium mobilization, which is a hallmark of chemokine receptor activation. Relevance of this antagonistic activity of CHIPS was shown as tumor cells had a strongly decreased chemotactic migration toward the aforementioned FPR1 agonists. Angiogenesis stimulation upon FPR1 activation was found to be inhibited by CHIPS. However, in a xenograft GBM mouse model no significant differences appeared in angiogenesis markers VEGF-A, Angiopoeietin-2 and Tie-2 between CHIPS treated and untreated tumors. Both in vitro and in a mouse xenograft model, no inhibition of proliferation was found. The percentage of the cleaved caspase-3 positive cells in the normoxic area of the xenograft tumor differed significantly from each other, although this was a small difference. Overall CHIPS treatment did not lead to significantly reduced tumor volume, although the median survival of CHIPS treated animals was significantly higher (Boer et al., 2013).

The astrocytoma cell line U87 has already been cultured for an extensive amount of time, in which it may have lost the true characteristics of GBM cells. This might be the reason of the existing discrepancy in literature considering the role of FPR1 in GBM. To obtain a more reliable and relatable cell line a number of primary patient derived GBM cell lines were obtained (the GG cell lines). Unexpectedly, out of 12 tested, only one of these cell lines, GG5, showed functional FPR1 expression. This is surprising because FPR1 is expected to be found in the great majority of GBMs.

Research question

Why do the majority of the GG cell lines not express FPR1? Answering this question is the first and main goal of this research. We investigated two possible reasons for this lack of expression.

Phagocytic leukocytes are known to heavily infiltrate GBMs (Yang et al., 2010). The cultured cells arise from tumor stem cells and not from tumor associated macrophages which may be the reason that so few cell lines show FPR1 expression. Therefore we investigated whether the FPR1 expression in GBM tissue can actually be completely attributed to the activity on the phagoctyic leukocytes.

CD68 is a commonly used marker of monocytes and macrophages (Song et al., 2011). Within tumors, one type of macrophages can in some cases be beneficial for tumor growth; these cells are known as M2 macrophages and are distinguished from M1 macrophages by their CD163 expression (Heusinkveld and van der Burg, 2011). GFAP is a well known marker of astrocytes (Cullen et al., 2007; Jacque et al., 1978), thus in the context of this study as a marker of the fast-dividing tumor cells. To answer the question whether FPR1 in glioblastoma is only expressed on macrophages, a double staining was performed with CD68, CD163 or GFAP.

Another explanation of the loss of FPR1 expression in the GG cell lines may be that FPR1 expression may be stimulated by the tumor microenvironment. When these cells are cultured, they may lack the necessary signals from the environment that stimulate FPR1 expression. This principle has been shown before; CXCR4 expression for example is upregulated in human skin melanoma when treated with a demethylating agent or a HDAC inhibitor (Mori et al., 2005). It may be that factors derived from untreated GBM may be sufficient to resurface the expression of FPR1. To investigate this question, first the FPR1 expression on the patient GBM tissues out of which the GG cell lines originated was determined. Secondly, these cultures were implanted into mouse brains and we evaluated the FPR1 expression in mouse xenograft tumor specimens obtained from the implanted GG cell lines.

The second aim of this project was to evaluate CHIPS treatment in the GG5 cell line. We investigated whether CHIPS would have a different effect in the more reliable and relatable GG5

FPR1 positive cell line than in the U87 cell line. It was chosen to investigate this because of the discrepancy between the results of the implanted U87 in mice (Boer et al., 2013) and previous studies (Yao et al., 2008; Zhou et al., 2005). GG5 cells were subcutaneously implanted in non-obese diabetic/ severe combined immune-deficient (NOD/SCID) mice. Treatment with CHIPS did not significantly affect the tumor size or survival. To investigate the characteristics of these tumors, the levels of angiogenesis (Ang-1, Ang-2, Tie-2), proliferation (Ki67) and apoptosis (cleaved caspase-3) markers were determined. This data was also compared with the proliferation and apoptosis data of the previous study of Boer et al on mouse xenografts of U87 cells.

Finally, also the extent of FPR1 expression in human glioblastoma was examined by staining a large number of patient glioblastoma tissues. The level of FPR1 expression found on these tumors was correlated with their molecular subtype (classic, proneural, neural, mesenchymal).

Material and methods

FPR1 expression of human GBM

To detect differences in FPR1 expression in human GBM tissue and animal xenografted tumor tissue was snap-frozen or formalin fixed and paraffin embedded (FFPE) and stained for FPR1. This staining was performed on snap-frozen human patient glioblastoma tissue of 36 patients (excluding tissues of five patients that were too thin). Some patients had multiple parts of tumor tissue and consequently 44 tissues were cut. FPR1 staining was also performed on a tissue micro-array (TMA) of 128 human FFPE tumors (4 cores per patient).

GG5 and the xenograft GBM mouse model

To study the effects of CHIPS treatment on the GG5 GBM cell line *in vivo*, 9 NOD/SCID mice were subcutaneously implanted in the dorsal flank with 5 x 10^6 GG5 cells in 100 µL PBS. Culturing tumor stem cells of a GBM (T11-10551) has resulted in the GG5 cell line, which was the only one of 12 GG cell lines expressing functional FPR1. The randomly assigned treated group (n=6) received E. coli derived CHIPS (intraperitoneal injections with 0.3 mg/kg once daily), the control group (n=3) received injections of equal volumes of PBS. After reaching the humane endpoint (tumor size ≥ 2 cm^3), the mice were sacrificed. The experimental procedure was approved by the Institutional Animal Care and Use Committee (IACUC) and conducted with institutional ethical regulations for experimental animal care.

To explore influence of CHIPS treatment, snap-frozen or FFPE tissues of 9 mouse xenograft tumors were stained for several markers. Angiogenesis in these tumors was studied by staining for angiopoietin-1, angiopoietin-2 and Tie-2 on snap frozen tissue. Ki67 was used as a proliferation marker and cleaved caspase-3 as apoptotic marker on the FFPE tissue. To distinguish normoxic from hypoxic areas, the hypoxia marker glucose transporter 1 (GLUT-1) was used. A staining for FPR1 expression was also performed on both snap frozen and FFPE tissues.

Immunohistochemistry

The frozen tissues were cut into 4 µm sections and which were mounted on Starfrost® adhesive slides and were stored in tinfoil at -20° C. After drying slides for 20 minutes under a cold hairdryer, the frozen-cut tissues were fixed in acetone for 10 minutes and then washed with PBS (PBS, 2.7 mM KCl, 1.8 mM KH_2PO_4, 137 mM NaCl, 10.1 mM Na_2HPO_4, pH 7.4). The sections were incubated with the primary antibody diluted in 1% Bovine Serum Albumin (BSA)/ PBS at room temperature (RT) for 1 hour. Subsequently, endogenous peroxidase was blocked with 0.33 % H_2O_2 in PBS for 30 minutes. After washing, the slides were incubated with the secondary antibody in 1% BSA/ PBS + 1% AB serum for 30 minutes. After again washing, the slides were incubated with the tertiary antibody in 1% BSA/ PBS + 1% AB serum for 30 minutes and were then once again washed with PBS. The AEC (3-Amino-9-Ethylcarbazole) reaction for 15 minutes was used for color development. Finally, slides were then washed in demi-water, counterstained with hematoxylin for 2 minutes and rinsed with tap water and mounted with Kaiser's glycerol-gelatin.

Prior to staining, the formalin fixed, paraffin embedded slides (4 µm thick) were deparaffinised in xylol (2 x 5 minutes) and rehydrated in a graded alcohol series. Endogenous peroxidase was blocked with 0.33 % H_2O_2 in PBS for 30 minutes. Subsequently, antigen retrieval was performed

in a preheated buffer (table 1) for 15 minutes in a microwave, followed by 15 minutes of cooling down and washing with PBS. Sections were incubated with the primary antibody diluted in 1% BSA/ PBS at room temperature (RT) for 1 hour or at 4° C overnight. After washing, incubation of the secondary and tertiary antibody was performed (table 1). Antibody binding was detected by a *3,3' diaminobenzidine (DAB) system.* Slides were then washed in demi-water, counterstained with hematoxylin for 2 minutes, rinsed with tap water. The FFPE slides were dehydrated by 3 alcohol steps and covered by a covering machine.
For each staining, omission of primary antibody and an appropriate preparation of control IgG (when possible) served as a negative control.

Primary antibody	Tissue	Clone	Donor	Manu-facturer	AR	DP	2nd antibody	DS	3rd antibody	DT
FPR1 (FFPE)	Human TMA	Poly-clonal	Rabbit	Abcam	Tris-HCl	1:250 (ON)	GARpo	1:100	RAGpo	1:100
FPR1 (FFPE)	Xenograft in mouse	Poly-clonal	Rabbit	Abcam	Tris-HCl	1:250 (ON)	GARpo	1:100	RAGpo	1:100
FPR1 (F)	Human	Poly-clonal	Rabbit	Abcam	None	1:600 (RT)	GARpo	1:100	RAGpo	1:100
FPR1 (F)	Xenograft in mouse	Poly-clonal	Rabbit	Abcam	None	1:600 (RT)	GARpo	1:100	RAGpo	1:100
Angiopoietin-1 (F)	Xenograft in mouse	Poly-clonal	Goat	Santa-Cruz	None	1:100 (RT)	RAGpo	1:100	GARpo	1:100
Angiopoietin-2 (F)	Xenograft in mouse	Poly-clonal	Goat	Santa-Cruz	None	1:50 (RT)	RAGpo	1:100	GARpo	1:100
Tie-2 (F)	Xenograft in mouse	Poly-clonal	Rabbit	Santa-Cruz	None	1:50 (RT)	GARpo	1:100	RAGpo	1:100
Ki67 (FFPE)	Xenograft in mouse	M724 0	Mouse	DAKO	Tris-EDTA	1:300 (RT)	RAMpo	1:100	GARpo	1:100
Cleaved caspase-3 (FFPE)	Xenograft in mouse	Poly-clonal	Rabbit	Cell Signal-ling	EDTA	1:100 (RT)	GARpo	1:50	RAGpo	1:50
GLUT-1 (FFPE)	Xenograft in mouse	Poly-clonal	Rabbit	Milli-Pore	Tris-HCl	1:750 (RT)	GARpo	1:100	RAGpo	1:100
CD68 (FFPE)	Human	PGM1	Mouse	DAKO	Tris-HCl	1:100 (ON)	RAMpo	1:100	GARpo	1:100
CD163 (FFPE)	Human	NCL	Mouse	Leica	Tris-HCl	1:100 (ON)	RAMpo	1:100	GARpo	1:100
GFAP (FFPE)	Human	6F2	Mouse	LSbio	Tris-HCl	1:50 (ON)	RAMpo	1:100	GARpo	1:100

Table 1: the antibodies used for staining. (FFPE) = formalin fixed, paraffin embedded. (F) = frozen. (AR) = type of antigen retrieval buffer. (DP) = dilution of primary antibody. (DS) = dilution of secondary antibody. (DT) = Dilution of tertiary antibody. (GARpo) = Goat anti-Rabbit horseradish peroxidase. (RAGpo) = Rabbit anti-goat horseradish peroxidase. (RAMpo) = Rabbit anti-Mouse horseradish peroxidase

Doublestaining

Doublestainings were performed with FPR1 and several cell type markers on human GBM tissue. CD68, CD163 and GFAP concentrations were optimized using DAB staining on human GBM tissue (FFPE), human tonsil tissue served as positive control (see fig. 1); for FPR1 the same concentration was used as on the FFPE human GBM tissues (1:250, 4° C, overnight). CD68, CD163 and GFAP stainings were optimized with Tris-HCl as antigen-retrieval buffer to match the FPR1 staining conditions.

Tissues intended for doublestaining were deparaffinized, antigen retrieval in Tris-HCl buffer was performed and they were washed in PBS. Subsequently, slides were blocked with 1% BSA/PBS for 30 minutes, to block unspecific antibody binding. After PBS washing, slides were incubated with a mixture of FPR1 and the marker (CD68, CD163 or GFAP) in 1% BSA/PBS and stored at 4° C overnight. Slides were then washed in PBS and incubated with a mixture of two secondary antibodies for 1 hour (1:400 goat anti mouse (Alexa 488), 1:400 goat anti rabbit (Alexa 647). After secondary antibody incubation, the slides were washed three times with PBS for 5 minutes each in the dark, stained with DAPI (1:2500) for 5 minutes, washed three times 5 minutes in PBS and mounted with 50 µL of Vectashield®.

Scoring

Digital images of all IHC slides were obtained by Aperio ScanScope CS Slide Scanner (Aperio Technologies Inc., CA, USA) under 200x or 400x magnification. Digital slides were analyzed with ImageScope v11.1.2.752 viewing software (Aperio Technologies).

The 200 x magnification digital slides were visualized in Imagescope. A distinction was made between a normoxic and a hypoxic area of the mouse tumor slides. FPR1 on frozen human tissue and Ki67 and cleaved caspase-3 on paraffin embedded mouse tissue were scored by counting the percentage of positive cells. For FPR1 for frozen human tissue, 5 random high power fields (200 µm by 200 µm) were chosen; Ki67 and cleaved caspase-3 were scored in 3 random high power fields in the normoxic area and 3 in the hypoxic area. First the total cell number in this field was counted; next the number of positive cells was counted to calculate the percentage of positive cells. A cell was considered positive when it shows more staining than the background level, which was determined by looking at a necrotic area. For FPR1 on frozen human tissue, the antigenic load was also determined, by multiplying the percentage of positive cells with an overall intensity score of the positive cells in that field. A negative field was given a score of 0, while a very strongly positive field got a score of 4.

The FPR1 expression on the human GBM TMA was evaluated by using a scale of 0-3, in which 0 corresponds with a negative core and 3 with a diffuse dark staining. As completely necrotic cores were left out of the scoring procedure, the average was taken of the remaining cores to obtain the average score of the patient. This scoring was done by two independent observers. These results were compared with results of clustering 128 of these tumors in 4 subtypes (and one group containing GBMs that could not be fitted in one of these 4 subtypes). Immunofluorescent slides were visualized with a Leica DM 600 B microscope and a Leica DFC360 FX camera and were evaluated and pictured using Leica Application Suite Advanced Fluorescence (LAS AF) software, version 2.5. Magnification: ocular 10x, objective 40x and a additional 1.6 magnification resulting in a total of 640x magnification.

We used fluorochrome Alexa 647 to visualize the more diffuse FPR1 staining, because GBM tissue is mainly autofluorescent in the filter for fluorochrome Alexa 488. CD68, CD163 and GFAP were easier to distinguish from this autofluorescence compared to FPR1. A relatively high exposure time and light intensity was necessary to identify FPR1 staining, compared to the exposure time and light intensity for CD68, CD163, GFAP or DAPI.

Statistics

Data are presented as averages with standard error. A 2-tailed p-value of 0.05 or lower was considered significant. Statistics on the non-parametric Ki67 and cleaved caspase-3 data were performed with the Mann-Whitney U test. Statistics on glioblastoma subtyping were done with a Kruskal-Wallis test. Graphs and statistic analyses were made with GraphPad Prism (version 5.00 for Windows, GraphPad Software, San Diego California USA, www.graphpad.com).

Results

FPR1 expression in patient glioblastomas

Due to extensive necrotic areas and bad morphology of frozen GBM tissues, one patient could not be properly scored. All remaining 35 patients showed FPR1 expression, with the percentage positive cells ranging from 19% to 63% (see fig 2). The average percentage of positive cells is 34.77 % ± 11.16 %. The FPR1 positivity was very heterogeneous within a tumor, as some fields of view were almost completely negative while the FPR1 percentage of other fields approached 100. No significant correlation was found between the percentage of positive cells or the antigenic load with patient survival, see fig 3.

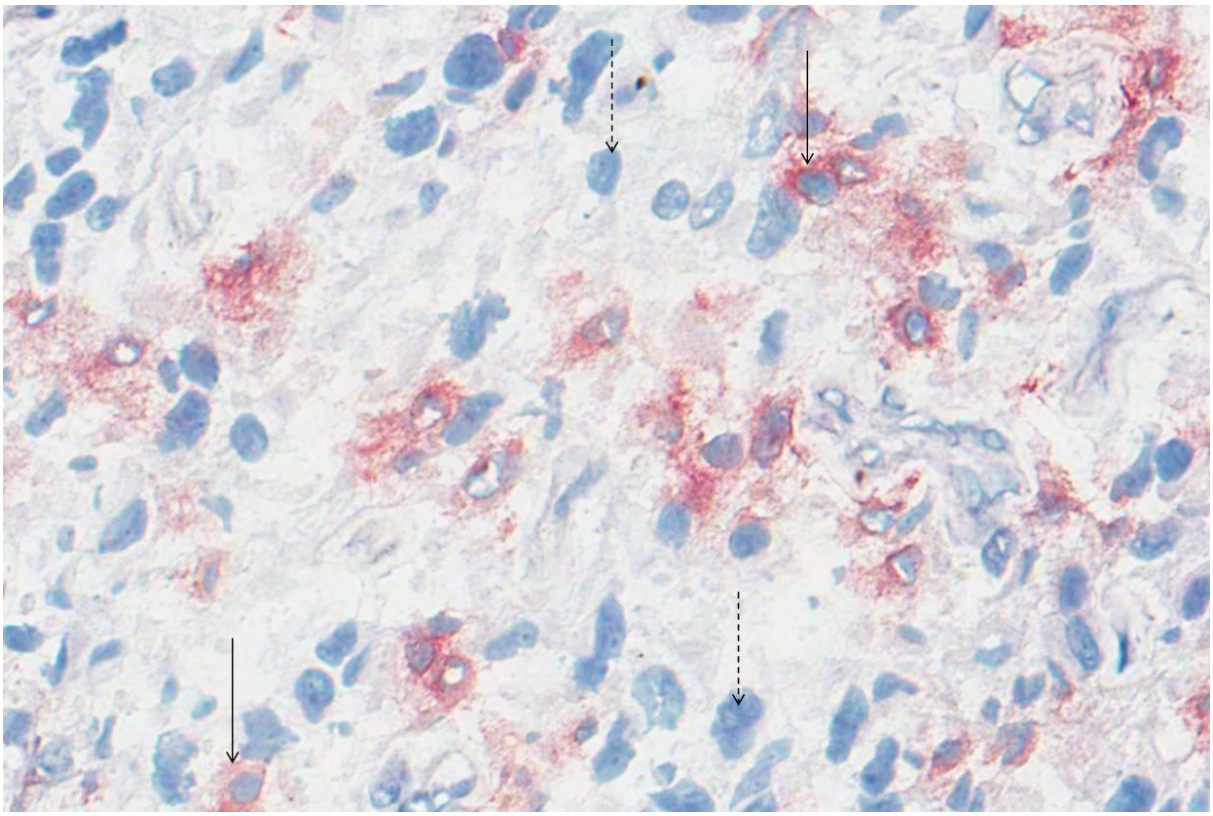

Fig 2: FPR1 expression on human GBM tissue (magnification of digital image: 400x). The continuous arrows indicate examples of FPR1 positive cells, the dashed arrows point out FPR1 negative cells. Average percentage of FPR1 positive cells on this tissue is 28% ±5.8%, antigenic load is 66.

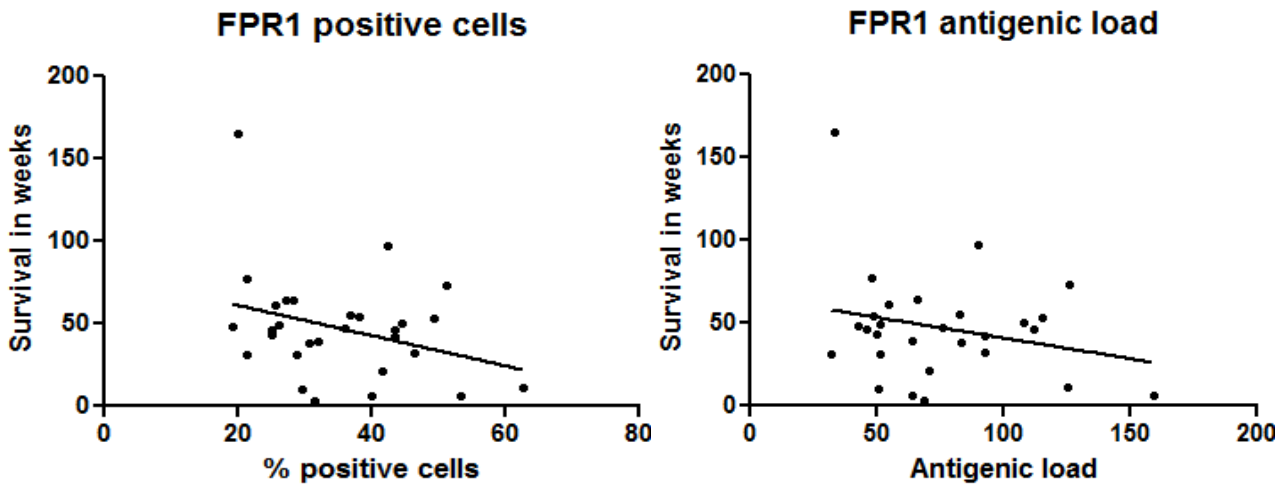

Fig 3 A: the percentage of FPR1 positive cells on snap frozen human GBM tissue plotted against patient survival after diagnosis (in weeks). Survival data of only 29 patients were available and thus plotted. The r^2 value of the regression line is 0.1030, the slope is not significantly non-zero, although al trend towards a negative correlation between FPR1 positive cells and survival is shown (p=0.0895). Fig 3 B: antigenic load of FPR1 in snap frozen human GBM tissue plotted against patient survival after diagnosis (in weeks). The r^2 value of the regression line is smaller than that of the percentage positive cells: 0.0592. The slope does not differ significantly from zero (p=0.2033).

FPR1 expression was also tested on human formalin fixed, paraffin embedded GBM tissue. This antibody gave a more diffuse staining, as is shown in fig 4. Although some cores were scored negative for FPR1, none of the patient GBMs had 4 FPR1 negative cores. The distribution of the GBMs among the 4 FPR1 expression groups is shown in table 2. The data from these tumors were matched with the 128 clustered GBMs (fig 5). Only 52 of the 128 GBMs could be clustered in one of the 4 subtypes, the other 76 GBMs were grouped as 'others'. The proneural (n=10) and mesenchymal (n=10) subtypes tended to have higher levels of FPR1 expression than the classic (n=25) and neural (n=7) subtypes, but A Kruskal-Wallis test did not provide statistic evidence for this observation.

FPR1 expression scores on human GBM TMAs	
Average score	Number of GBMs
0-0.5	0
0.5-1.5	39
1.5-2.5	58
2.5-3.0	31

Table 2: the expression of FPR1 on 128 patient GBMs on a TMA. This table shows the average score of four cores per tumor, scored by two independent observers. No GBM had an average score of 0.5 or lower.

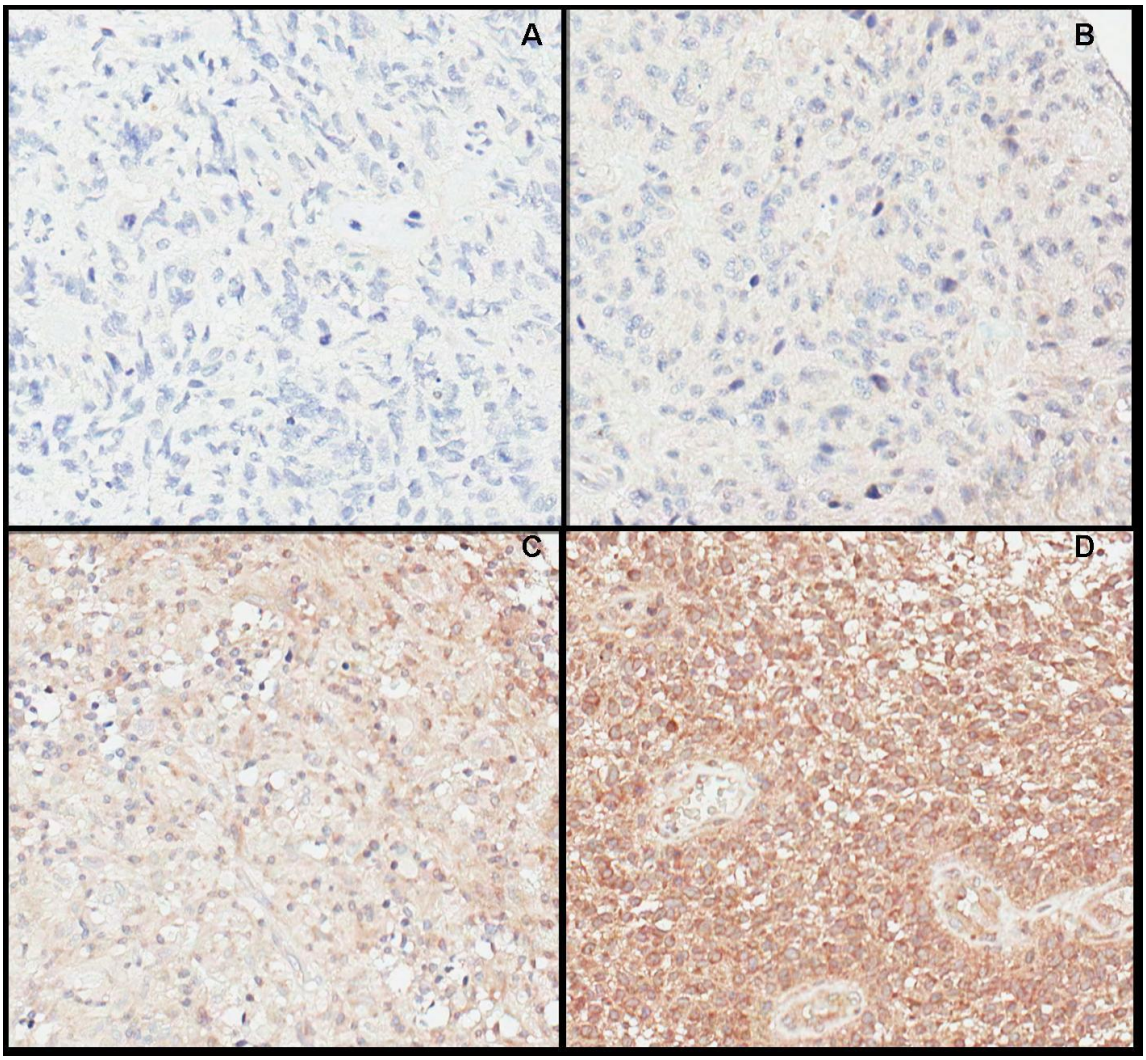

*Fig 4: FPR1 expression on human GBM on a TMA (magnification of digital image 200x). The GBM cores were scored 0 (**A**), 1(**B**), 2 (**C**) or 3 (**D**). In the FPR1 positive cores, a diffuse background can be found and a more intense staining closer to the nucleus. Especially in the higher categories, 100% of the cells seem positive for FPR1. The GBM tissue shown in **B** is the same as the one shown in fig 2.*

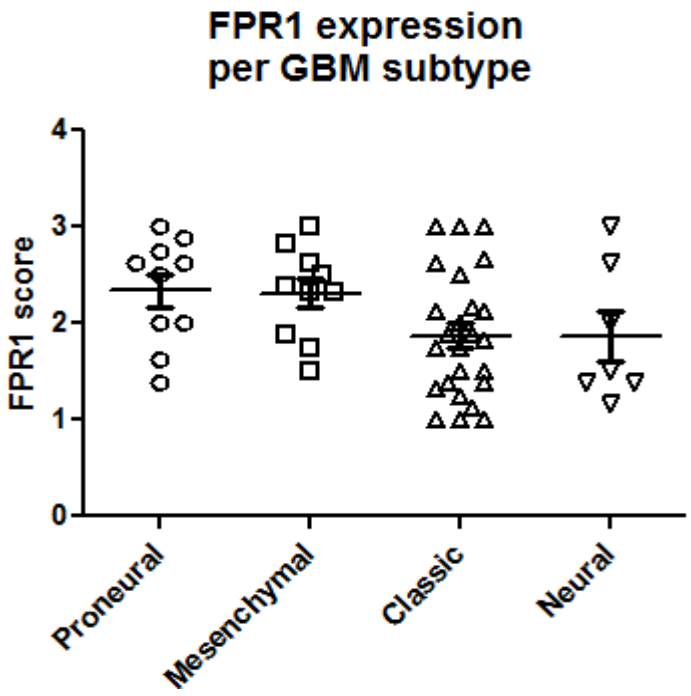

Fig 5: expression of FPR1 scored on GBM TMA matched with the according GBM subtypes. The average score is shown ± SEM. The proneural (2.338 ± 0.175) and mesenchymal (2.313 ± 0.151) seem to have a higher FPR1 score compared to the classic (1.870 ± 0.129) and neural (1.863 ± 0.267). A Kruskal-Willis test did not show significant differences between the groups (p=0.1037).

FPR1 staining on GG cell lines implanted in mouse brains

The GBMs out of which the GG cell lines showed almost all FPR1 expression, some were even scored with a 3. Only one tissue was scored negative, but this was a very small part of tissue. All five mouse brain tumors originated from five different GG cell lines showed FPR1 expression. The tumors differed in their anatomical presentation, but for every tumor specific FPR1 expression was found, probably also on astrocyte tumor cells (see fig 6).

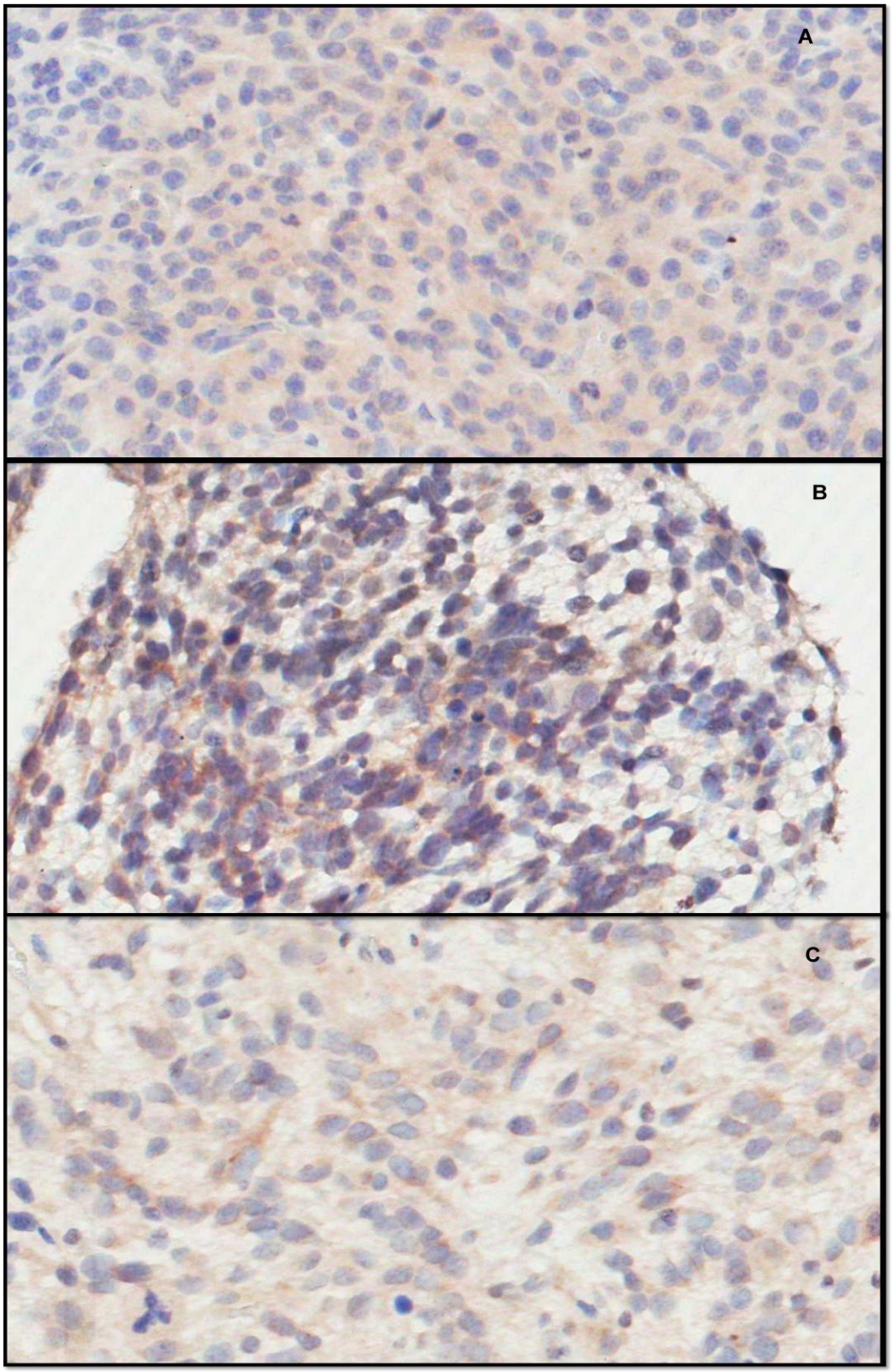

*Fig 6: Three examples of FPR1 expression detection by DAB system in implanted GBM cell lines in mouse brains. **A** shows a GG5 tumor, **B** shows a GG13 tumor residing in the ventricle and **C** shows a GG16 tumor, which had invaded the meninges. Magnification: 400x*

Doublestainings

Doublestainings were performed on human GBM tissue to identify which cells express FPR1. FPR1 is found to be co-expressed with CD68, CD163 and GFAP (see fig 7 and 8). In accordance with the DAB staining on the FFPE tissue, but not with the staining on the snap frozen tissues, most tissues showed FPR1 expression in all cells. This made it impossible to find CD68 and CD163 single positive cells. GFAP single staining seemed to be found in some rare cases.

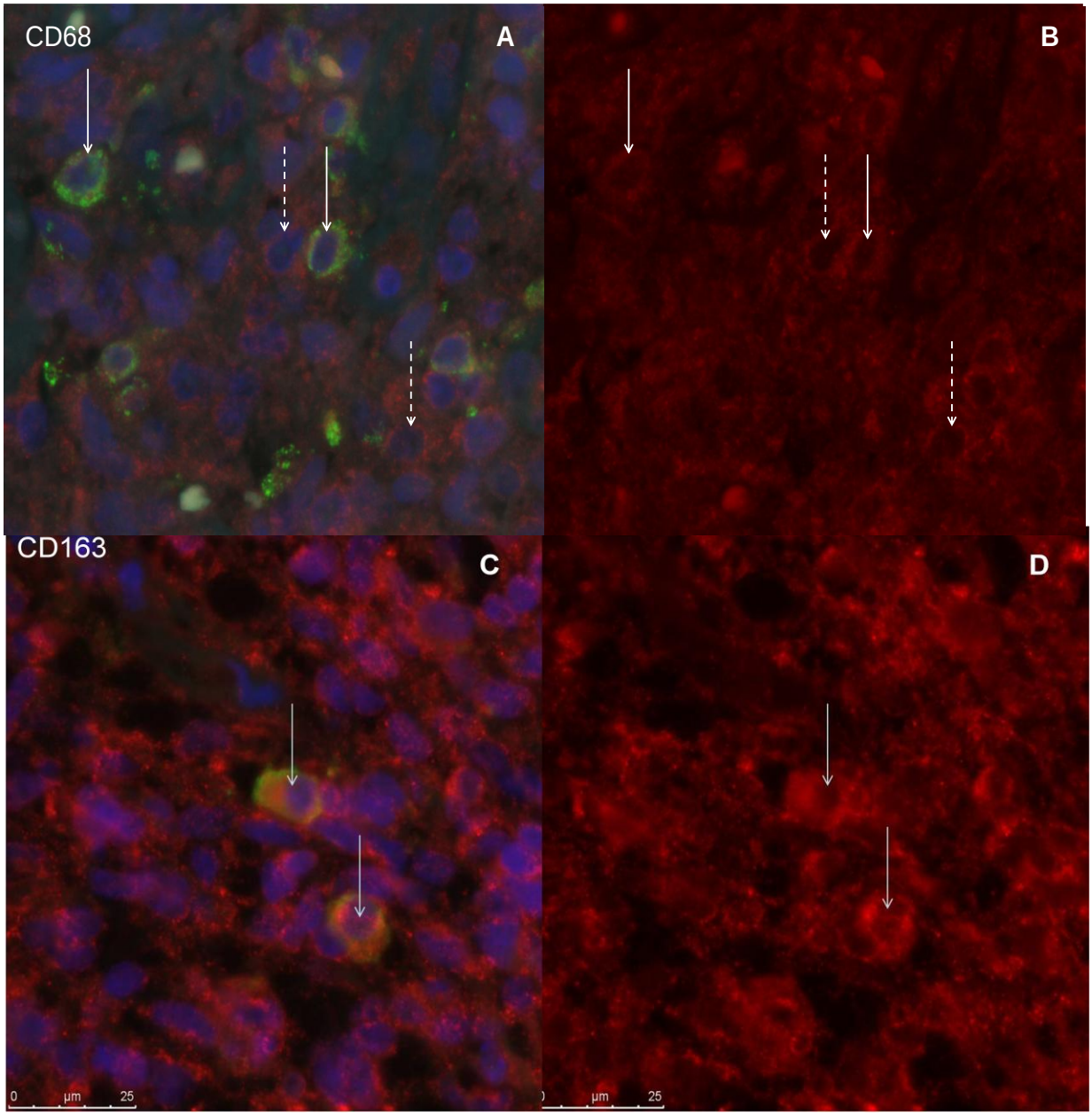

*Fig 7: Overlay (**A and C**) pictures of examples CD68 and CD163 doublestaining with FPR1. Next to these overlay pictures, a picture of the red filter in the same region is shown, which corresponds with the FPR1 expression (**B** and **D**). Continuous arrows indicate CD68 or CD163 coexpression on a cell with FPR1. Dashed arrows indicate FPR1 single staining. The example of the CD68 doublestaining (**A** and **B**) with FPR1 shows a less intense FPR1 staining than that of CD163 (**C** and **D**), but in both examples 100% of the cells seem to express FPR1. Magnification 640x*

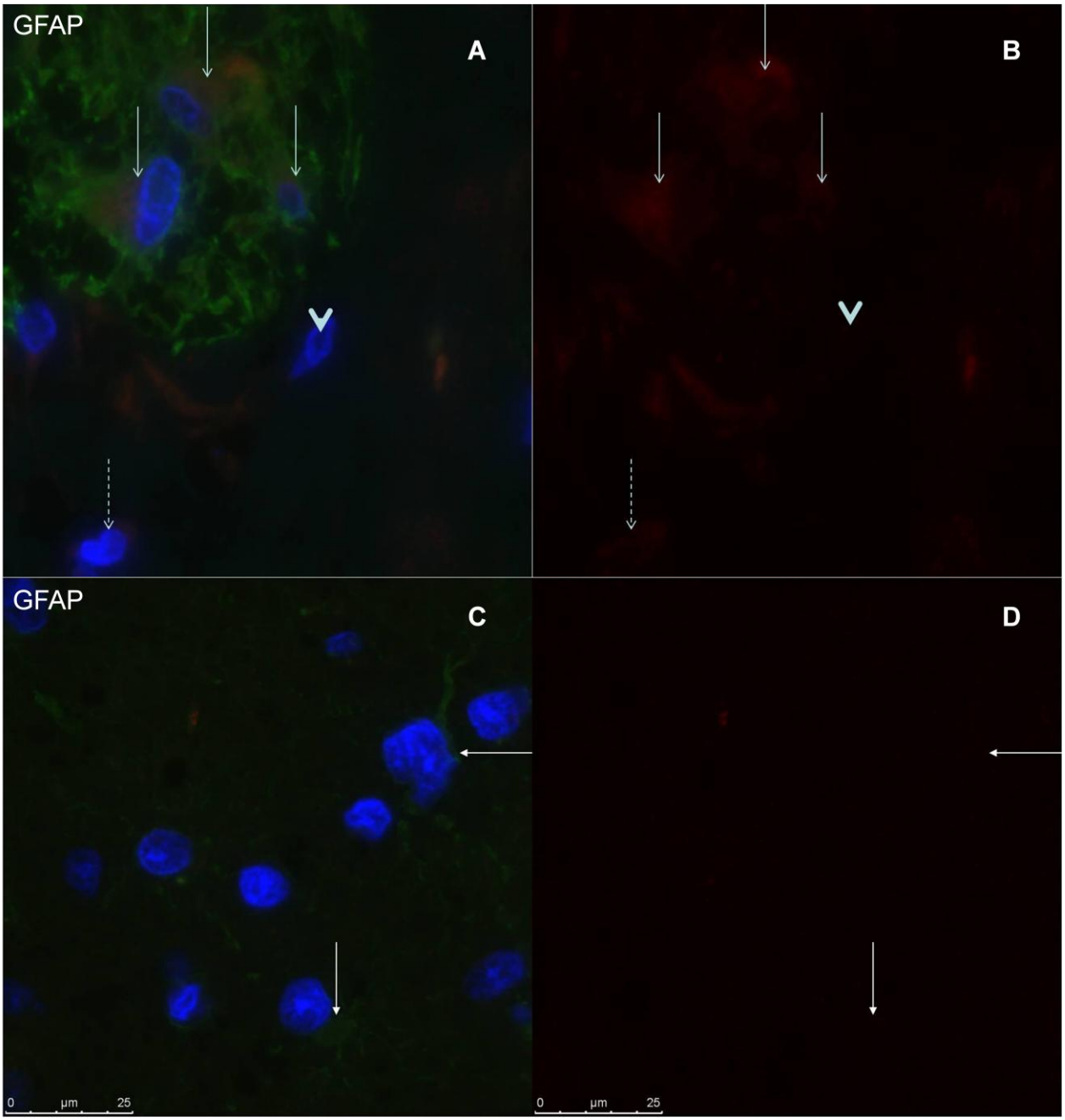

*Fig 8: Overlay (**A and C**) pictures of examples GFAP doublestaining with FPR1. Next to these overlay pictures, a picture of the red filter in the same region is shown, which corresponds with the FPR1 expression (**B** and **D**). Continuous arrows indicate GFAP coexpression on a cell with FPR1. Interrupted arrows indicate FPR1 single staining. An arrowhead indicates a FPR1 and GFAP negative cell. Figure **C** and **D** were taken from a tissue that showed moderate FPR1 staining at some places of the tissue, while the pictured part of the tissue seemed to be largely FPR1 negative. Magnification 640x*

GG5 mouse xenograft

The xenograft tumors in the mice originated from the FPR1 positive glioblastoma cell line GG5. We investigated whether these tumors were also FPR1 positive and whether CHIPS treatment altered FPR1 expression and angiogenesis, proliferation and apoptosis markers. Using GLUT-1 staining and differences in the morphology on the tissue, a distinction could be made between normoxic and hypoxic regions of the tumors.
FPR1 staining on snap frozen and FFPE tissue is shown in fig 9. No obvious differences in FPR1 expression were found between CHIPS treated (n=6) and untreated (n=3) animals.

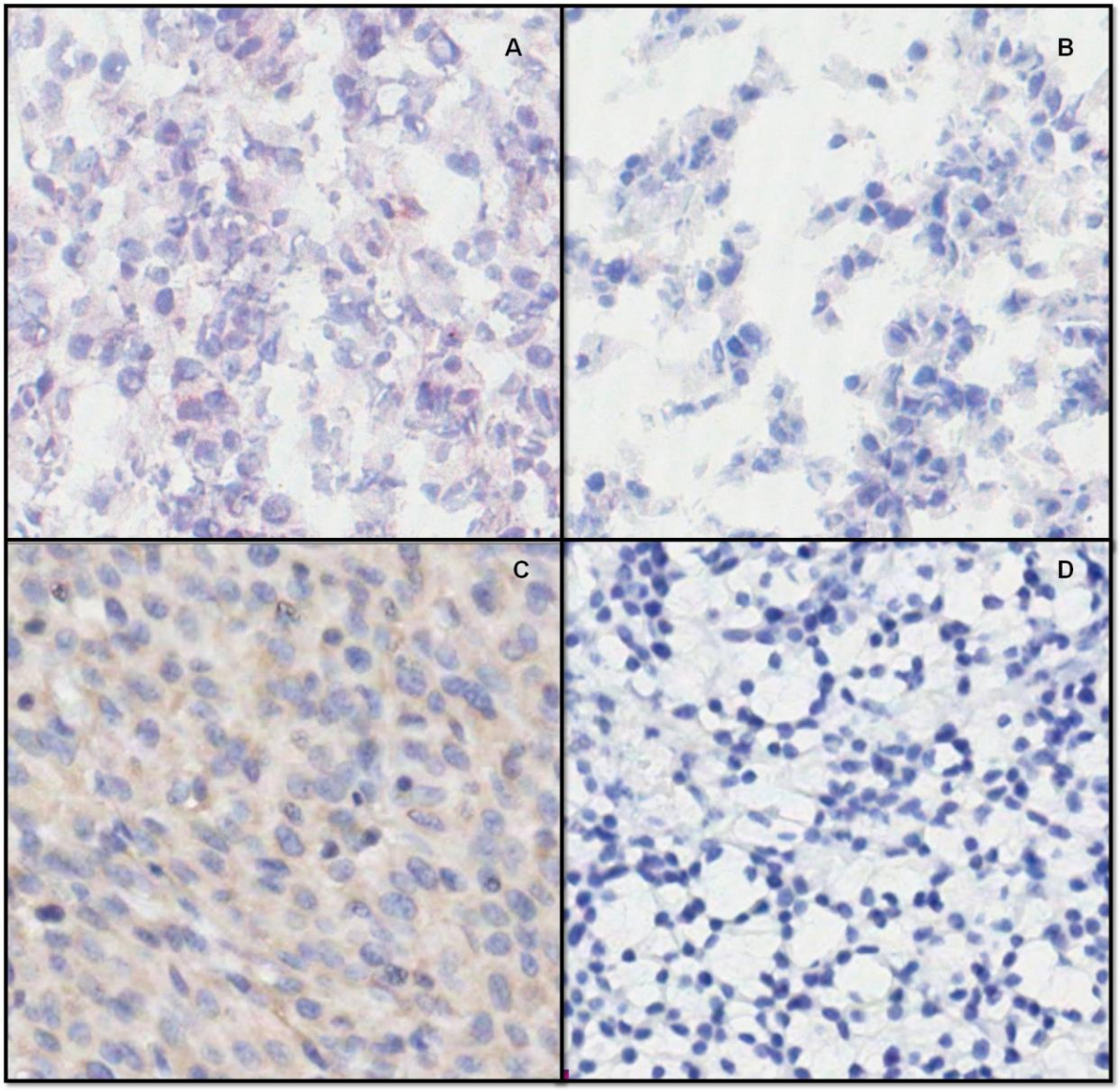

Fig 9: FPR1 expression on mouse xenograft tumor originated from the glioblastoma cell line GG5 (all pictures are from the same animal). ***A*** *shows the result of an AEC reaction in a normoxic region of a snap frozen tumor and* ***B*** *shows the result of this reaction in a hypoxic region of a snap frozen tumor.* ***C*** *shows the result of a DAB reaction in a normoxic region of a FFPE tumor and* ***D*** *shows this reaction in a hypoxic region of a FFPE tumor. Magnification of digital image 400x*

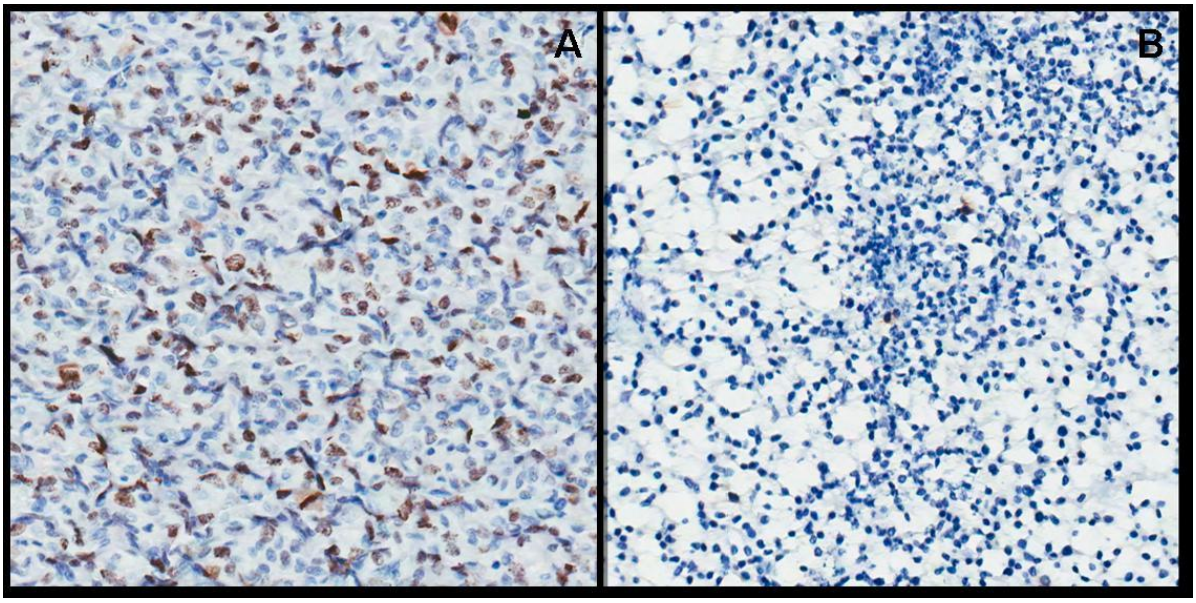

*Fig 10: Ki67 staining on FFPE (CHIPS treated) mouse xenograft tumor. A normoxic region is shown in **A**, a hypoxic region is shown in **B**. Magnification 200x*

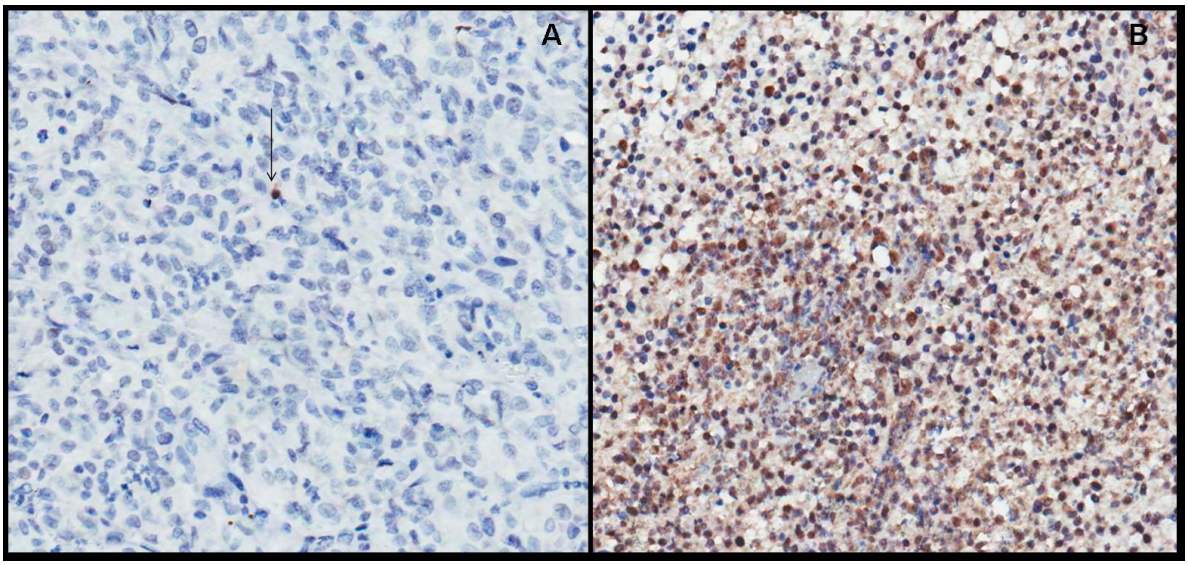

*Fig 11: Cleaved caspase-3 expression on a FFPE (CHIPS treated) mouse xenograft tumor. **A:** In the normoxic zone, the percentage of positive cells is very low. The arrow points at a sole cleaved caspase-3 positive cell. **B:** The expression is clearly higher in the hypoxic zone. Magnification 200x*

Angiogenesis in these tumors was examined by staining with angiopoeietin-1, angiopoeietin-2 and Tie-2 on frozen tissue. No observable differences could be found between CHIPS treated and untreated animals; it was decided not to score these slides.

Ki67 staining was performed to visualize the level of proliferation in the FFPE tumors. An example of Ki67 staining in a normoxic and a hypoxic area is shown in fig 10. As this figure clearly shows, the expression of Ki67 differs significantly between the normoxic and the hypoxic region of the tumor. The difference between CHIPS treated and untreated animals does not reach significance, both in the normoxic and the hypoxic zone. The previously scored U87 tumors had in both regions a higher percentage of positive cells compared to GG5 tumors (fig 12).

An example of a staining with the apoptotic marker cleaved caspase-3 is shown in fig 11. The normoxic region had a very low percentage of positive cells, this differed significantly from the percentage cleaved caspase-3 positive cells in the hypoxic region. A Mann-Whitney test showed no significant differences between cleaved caspase-3 expression in the normoxic or hypoxic regions of CHIPS treated animals versus untreated animals (see fig 12). Cleaved caspase-3 expression tended to be higher in GG5 tumors compared to U87 tumors, this difference approached significance.

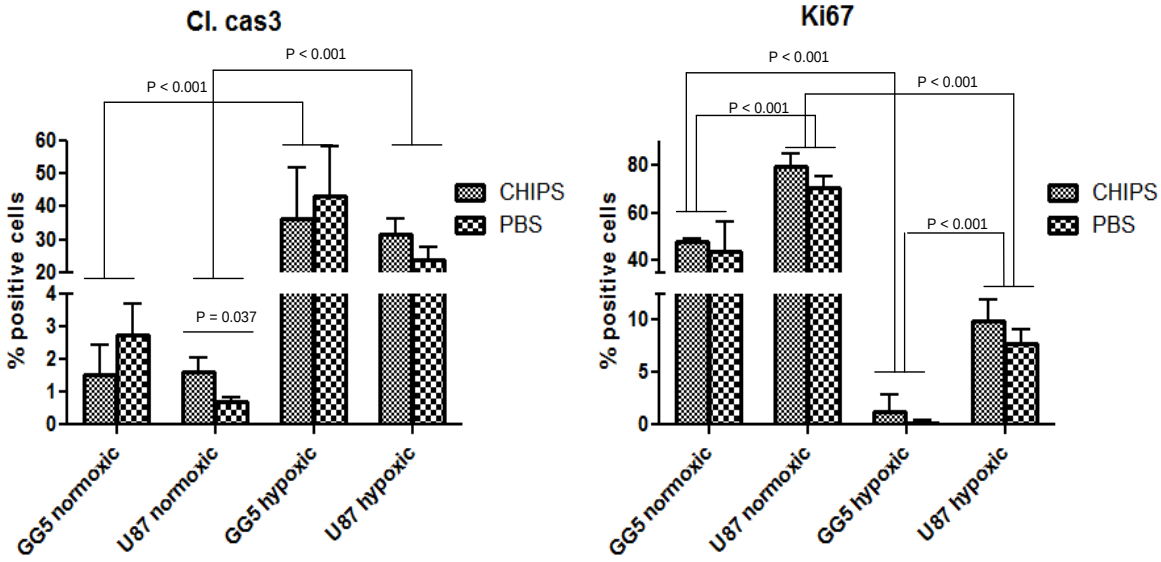

Fig 12: percentage of positive cells in the normoxic and hypoxic region of the mouse xenograft GG5 and U87 tumors.

***A:** For both GG5 and U87 tumors the Ki67 expression differs between the hypoxic and normoxic zone (p<0.001 for GG5 and for U87). Expression differences can't be found (in either normoxic or hypoxic areas) in CHIPS treated versus untreated animals of both tumor types. More Ki67 positive cells were scored in U87 tumors compared to GG5 tumors (p<0.001 for both normoxic and hypoxic).*

***B:** Cleaved caspase-3 expression is significantly higher in the hypoxic zone (p<0.001 for GG5 and for U87). U87 showed no differences in cleaved caspase-3 levels in the hypoxic zone (p=0.310), but did show a significant increase in expression for the treated group in the normoxic zone (p=0.037). In GG5 tumors on the other hand, no significant differences in the percentage of positive cells could be found in the normoxic (p=0.167) or in the hypoxic zone (p=0.714). Cleaved caspase-3 activity tended to be higher in both the normoxic (p=0.07) and the hypoxic (0.08) zone of GG5 compared to U87.*

Discussion

This study focuses on the formyl peptide receptor 1 (FPR1), which is normally expressed on phagocytic leukocytes, but is more recently also found to be expressed in many glioblastomas. In this study, we found that the expression of FPR1 is widespread; all GBMs were positive at least to some extent for FPR1 and many tumors seem to consist for 100% of FPR1 positive cells.

Many previous studies showed FPR1 expressions in GBM (Boer et al., 2009; Zhou et al., 2005), but this study of 35 snap frozen and 141 FFPE GBMs (with a slight overlap) proves that almost every tumor shows to some extent FPR1 expression. The FPR1 expression was quite different in the snap frozen tissues (fig 2) compared to the FFPE tissues (fig 4). The FFPE staining for FPR1 used an antibody that is only recently on the market (Abcam, ab150533); yet no references are available of studies using this antibody. It may be that the antibody used on paraffin gives a less specific staining or that it binds to a different FPR1 epitope than the antibody used on snap frozen tissue (Abcam, ab101659). Unlike in FFPE tissues, epitopes in snap frozen tissues are not masked. During the FFPE process, fixed proteins may be coagulated and precipitated with organic solvents and by heating, which is responsible of the partially or completely masking of the epitopes. Heat-induced antigen retrieval is the most common used technique to retrieve the epitopes masked by the FFPE process. The pH of the antigen retrieval buffer is essential for optimal unmasking of epitopes; for most staining, basic buffers are known to be better in conserving tissue structures and unmasking epitopes than the acidic citrate buffer (Yamashita, 2007). The FPR1 staining was optimized for antigen retrieval buffers and unlike the Abcam datasheet stated, the basic Tris-HCl buffer (pH=9.0) gave better results than the citrate buffer (pH=6.0), although the differences were not that pronounced. It may be that in the FFPE process or during antigen retrieval, unspecific epitopes were formed diffusively in the cytoplasm of all cells. This may also be the cause of the difference in FPR1 expression on frozen or FFPE tissues.

There were many difficulties regarding the staining with the FPR1 antibody on paraffin tissue. As no results have been published of studies using this antibody, it was difficult to determine what the quality of the FPR1 stainings were and the concentration and antigen retrieval method had to be optimized. Staining on the same GBM tissue and positive control tissue gave different stainings, while none of the conditions had been changed. Because most other factors affecting stainings could be ruled out, these problems were likely caused by (the storage of) the antibody itself; repeated freeze-thaw cycles should be prevented. The FPR1 staining was very heterogeneous, which is not surprising, as GBMs are known to be histologically heterogeneous (DeAngelis, 2001). Scoring snap-frozen GBM tissue was in some cases problematic, as large parts of tumor comprised of necrosis.

No significant correlation was found between the percentage of FPR1 positive cells or the antigenic load on the 28 snap frozen human tissues with patient survival after surgery. Nevertheless, the percentage FPR1 positive cells seems to be negatively correlated with survival, as the regression analysis did show a trend. This could be explained by the fact that necrosis is correlated with lower survival (Sullivan and Graham, 2007; Yang et al., 2012); a high level of necrosis could provide higher levels of mitochondrial peptides that could be recognized by FPR1, so more FPR1 positive immune cells would migrate into the GBM tissue by chemotaxis.

The lack of FPR1 expression on the GG cell lines

The main goal of this research was to elucidate why all but one glioblastoma GG cell lines were negative for FPR1, while most, if not all, glioblastoma tissues are found to be FPR1 positive. One tissue, out of which a GG line was originated, was scored negative, but due to the very small size of this tissue it is not sure whether this is the case for the complete tissue.

One reason why FPR1 is not found in most of the GG cell lines, is that the FPR1 expression in GBM could almost completely be attributed to its presence on phagocytic leukocytes like macrophages. FPR1 is best known for its presence on these cells and these cells invade tumors like GBM to a high extent (Yang et al., 2010). M2 macrophages, distinguished from M1 macrophages by their CD163 expression, play normally a role in parasite clearance and dampen immune responses. In tumors, high numbers of these macrophages are thought to be beneficial for tumor growth and thus contribute to tumor malignancy (Carvalho da Fonseca and Badie, 2013; Heusinkveld and van der Burg, 2011). Various tumor-derived molecules are responsible for the drive of macrophages in the tumor towards a M2 phenotype (Komohara et al., 2008). A doublestaining of FPR1 with CD68, CD163 or GFAP was performed to determine on which cell type FPR1 is present. These proteins are markers of cell types that are expected to be found in GBM. CD68 is a macrophage (and lysosomal) marker and is highly expressed on mononuclear phagocytes (blood monocytes and tissue macrophages) (Yang et al., 2010). CD163 is used as a marker more specifically for M2 macrophages. Glial fibrillary acidic protein (GFAP) is involved in many central nervous system processes, including cell communication and maintaining astrocyte mechanical strength. GFAP is commonly used as a marker for astrocytes (Cullen et al., 2007; Jacque et al., 1978). FPR1 was found to be coexpressed with CD68 and CD163 in every cell, while also being expressed on the great majority of GFAP expressing cells. FPR1 was in most tissues actually expressed on every cell, although this expression was sometimes very light. This could be expected from observing the DAB staining of FPR1 on GBM on paraffin, which shows a quite diffuse specific staining on most (if not all) of the cells. The reliability of these stainings on paraffin tissue could be arguable, however staining performed on frozen tissue also shows FPR1 expression on circa 34 % of the cells. Observing the level of CD68 or CD163 positive cells in the doublestaining, it is almost impossible to attribute the FPR1 expression solely to infiltrated macrophages.

The FPR1 expression found on (M2) macrophages is expected, as macrophages are one of the first cell types on which FPR1 expression was found, before its discovery on GBM cells. However, FPR1 is not only expressed on (M2) macrophages but also on fast-dividing astrocyte tumor cells. Although not every tumor cell in every tissue seems FPR1 positive, the great majority of the GBM tissues show FPR1 on every single cell. These tissues could not provide FPR1 negative cells to be cultured. Therefore, the lack of FPR1 in the GG cell lines is not explained by culturing GBM cells that are FPR1 negative.

Another explanation for the loss of FPR1 on the GG cell lines, may be due to microenvironment-dependent FPR1 expression. We investigated this by examining whether implanting 5 GG cell lines resulted in resurfacing of FPR1 expression. We found in all these five tumors specific FPR1 staining.

Some of the brain tumors that resulted from the implantation of the GG cell lines were so diffuse that it was difficult to distinguish tumor cells from normal brain cells. Some cells in the brain do normally express FPR1, like neurons and ependymal cells (Becker et al., 1998). A combination with nestin staining may help to distinguish tumor cells from healthy cells (Tiede et al., 2007).

These findings suggest that FPR1 expression in GBM cells may depend on environmental factors. These factors are not present in cell culture, leading to FPR1 depletion until no functional FPR1 is expressed anymore. This is, to our knowledge, a rare phenomenon in which cells lack expression of a protein (and even its mRNA) in culture, while the expression resurfaces in an orthotopic mouse model. CXCR4 for example can be upregulated by environmental factors, but this always involves a type of treatment and in culture CXCR4 is still expressed on some level (Mori et al., 2005; Domanska et al., 2012). U87 and GG5 do still express FPR1 in cell culture, showing that environment-dependent FPR1 depletion cannot be applied in every case. It is yet unknown which factors are necessary for maintaining FPR1 expression, but the lack of FPR1 mRNA in culture indicates the possible involvement of soluable factors. The level of FPR1 expression on the GBM out of which the GG cell line originated seems not to be a factor that determines whether FPR1 is expressed on the GG cell line. GG5 for example shows only a light staining, while some FPR1 negative cell lines obtained the highest FPR1 expression score on the TMA.

Why is FPR1 not expressed on 11 of the 12 tested GG cell lines, while the GBMs where they originate from are probably all positive? Our data suggest that it is not because the FPR1 expression in GBMs is solely attributed to its expression on infiltrating phagocytic leukocytes. FPR1 is found on almost every astrocyte tumor cell, cells that were cultured must have expressed FPR1 before culturing. It has become clear that environmental factors are in most cases necessary for FPR1 to become expressed. This is shown as implantation of FPR1 negative cell lines in mouse brains leads to resurfacing of FPR1 expression.

GG5 xenograft tumors

Another goal of this research was to study the effects of CHIPS treatment on angiogenesis, proliferation and apoptosis on tumors that arose subcutaneously in mice after the implantation of GG5 cells. This part of this research is actually a repetition of the study performed earlier by Boer et al on U87 cells, where a treatment with CHIPS did not significantly affect angiogenesis and proliferation and had only a small effect on the apoptotic marker cleaved caspase-3 (Boer et al., 2013). Treatment with CHIPS, which is the most potent antagonist for FPR1 (Haas et al., 2004), was expected to have almost the same effect as FPR-siRNA treatment. FPR-siRNA was found to cause decreased tumor size, reduced proliferation rate, increased anti-apoptosis and reduced angiogenesis in GBM cells or in xenograft tumors (Yao et al., 2008; Zhou et al., 2005). Previously, in accordance with U87 xenograft tumors, CHIPS did not reduce tumor size significantly in GG5 tumors. Now, in this study, we show no differences in the angiogenic, proliferative and apoptotic markers between the CHIPS treated and untreated group.
The xenograft GG5 tumors contained extended hypoxic regions, but also necrotic regions. This unprogrammed cell death due to the rapid growing tumor mass is another hallmark of high grade astrocytomas, differentiating them from lower grade astrocytomas (Chen et al., 2013). Hypoxia is a state in which cells live with an oxygen deficiency and may precede necrosis. Hypoxia in tumors alters the expression of many proteins; important is the upregulation of angiogenic factors such as VEGF and HIF1α. These changes in expression due to hypoxia have consequences for the clinical outcome of GBM patients, as they cause a more malignant phenotype of cancer cells, recurrence of the tumor and a worse treatment response (Sullivan and Graham, 2007; Yang et al., 2012). Glucose transporter 1 (GLUT1) is one of these factors that is overexpressed in hypoxic areas of GBMs (Zhang et al., 1999). It was used in this study to help differentiating hypoxic from normoxic zones in the mouse xenograft tumors, although this was

sometimes difficult due to the relatively high expression of GLUT1 in the normoxic zone. Tie-2 and two of its ligands angiopoietin-1 and angiopoietin-2 are key actors in dictating vascular phenotype (stabilized or destabilized) and thus in angiogenesis. Hypoxia is known to alter the expression of these factors (Cascone and Heymach, 2012). FPR1 is suggested to play an important role in angiogenesis (Yao et al., 2008), therefore we hypothesized that CHIPS treatment may alter the Tie-2, angiopoietin-1 and angiopoietin-2 expression. This study showed no observable differences of the expression of those factors between CHIPS treated and untreated animals. This finding in GG5 xenograft tumors matches that of the U87 tumors implanted in mice by this group (Boer et al., 2013).

Evaluation of Ki67 and cleaved caspase-3 were done separately for the normoxic and hypoxic areas, as these factors are also expected to differ between these regions (Kuijlen et al., 2006). High proliferation is a prominent feature of GBMs (Louis et al., 2007), therefore expression of Ki67 was investigated, as Ki67 is a proliferation marker that is expressed in mitotic cells (Bowers et al, 2003). FPR1 activation is suggested to promote proliferation of GBMs (Yao et al., 2008; Zhou et al., 2005), so it might be that CHIPS treatment could decrease the expression of Ki67 in the tumor. But just like the previous study on U87 tumors, no effects could be found of the CHIPS treatment on Ki67 expression.

Proliferation is the factor that increases the cell number of tumors; apoptosis on the other hand, is a main factor that decreases the total cell number in tumors. Zhou et al did not only find an effect of FPR1 on proliferation but also on the anti-apoptotic marker bcl-2, but these results have not yet been corroborated. The study of Boer et al on U87 tumors did not show an effect of FPR1 blocking on bcl or on another anti-apoptotic protein, survivin. They did find a small but significant increase in the normoxic zone of the pro-apoptotic marker cleaved caspase-3. This increase was not found in the normoxic zone of the GG5 tumors from this study, as the expression of cleaved caspase-3 was actually (unsignificantly) higher in the treated group. The apoptotic marker expression in the hypoxic zone was neither different in U87 or GG5 tumors.

The data from GG5 tumors is found to show the approximately the same results of CHIPS treatment as that of U87 tumors. Significantly higher expression of Ki67 was scored in U87 tumors than in GG5 tumors. Cleaved caspase-3 expression was almost significantly scored higher in GG5 tumors than in U87 tumors, this difference was strong for untreated animals while the levels seemed the same for treated animals. These findings may indicate two things. Firstly, these differences could be attributed to the different observers of these tumors, as they might score in a systematically different way. If so, the levels of both markers should be higher for one observer. To find out if this causes these differences, one observer should (blindly) score both U87 and GG5 tumors. The second reason for the differences in Ki67 (and possibly cleaved caspase-3) could be that GG5 could indeed be characterized by less proliferation and possibly more apoptosis compared to U87. These two factors should lead to decreased tumor volume, although other factors could also be a main player in the determination of the speed of tumor growth. The volumes of the GG5 tumors at the end of the experiment were higher than that of U87 tumors, so it seems in this case that other factors determine the speed of tumor growth.

A future experiment on CHIPS treatment could focus on the invasion of tumor cells in the tissue surrounding the tumor tissue. GBM is known for its local invasion of surrounding brain tissue; only approximately 92% of GBM cells are found within the tumor core (Wang et al., 2013; Wilson et al., 1992). The remaining 8% of tumor cells invade the surrounding tissue and are found to have a distinct phenotype compared to cells in the tumor core (Giese et al., 2003). CHIPS is found to inhibit the migratory capacity of U87 cells upon fMLF stimulation in vitro (Boer et al., 2013). It could be investigated what effect CHIPS treatment has on the percentage of tumor cells at certain distances of the tumor core. Whether an inhibiting effect of CHIPS on

invasion *in vivo* has much therapeutic relevance is arguable, as at the time of diagnosis many tumor cells are expected to be migrated far away from the tumor core.

Concluding, this study shows no effect of treatment with the FPR1 antagonist CHIPS on angiogenesis, proliferation and apoptosis of GBM mouse xenografts. This is in accordance with the data on U87 mouse xenografts (Boer et al., 2013), but shows discrepancy with the study of Zhou et al in 2005 and Yao et al in 2008. These groups used siRNA, which is a different (and less therapeutically applicable) process than the use of an antagonist like CHIPS. These different methods may be responsible for the differences between these studies.

FPR1 and subtypes

We also investigated whether the variation of FPR1 expression levels, which differ from very light to very darkly diffuse, are correlated with the molecular subtypes of GBM. Many GBMs can be clustered in one of the 4 molecular subtypes: proneural, mesenchymal, classic or neural. The molecular subtyping of GBMs can predict certain characteristics of the disease and may be used in personalizing the treatment of GBM.
In this study we show no significantly different FPR1 expression score between the subgroups, although only less than 50% of the GBMs could be clustered,. The data does show a remarkably higher FPR1 expression of the proneural and mesenchymal subclasses. This is unexpected, as the other two subgroups are defined by EGFR amplification. EGFR amplification is a common feature of GBM and transactivation by FPR1 is calculated to account for approximately 40% of FPR1 malignancy (Huang et al., 2007). A higher number of clustered GBMs may provide more insight on this topic.

Conclusion

This study shows that FPR1 expression is a very common feature of GBM, as probably all GBMs show FPR1 expression. The finding that FPR1 is only expressed in the minority of cell lines is not due to low FPR1 expression in GBMs or the culturing of FPR1 negative cells out of a positive GBM, but because the environment in cell culture lacks factors that are necessary of FPR1 expression. We also found that, much alike U87 xenograft tumors, GG5 xenograft tumors show no effect of the FPR1 antagonist CHIPS on proliferation and apoptosis. No significant correlation was found between the expression of FPR1 and the molecular GBM subtype.

References

Abbas AK, Lichtman AH, Pillai S, 2010. Cellular and molecular immunology. 6th ed. Philidelphia: Elsevier Saunders.

Becker EL, Forouhar FA, Grunnet ML, Boulay F, Tardif M, Bormann BJ, Sodja D, Ye RD, Woska JR Jr, Murphy PM, 1998. Broad immunocytochemical localization of the formylpeptide receptor in human organs, tissues, and cells. Cell Tissue Res. Apr; 292(1): 129-35.

Boer JC, Domanska UM, Timmer-Bosscha H, Boer IG, de Haas CJ, Joseph JV, Kruyt FA, de Vries EG, den Dunnen WF, van Strijp JA, Walenkamp AM, 2013. Inhibition of formyl peptide receptor in high-grade astrocytoma by CHemotaxis Inhibitory Protein of S. aureus. Br J Cancer. 2013 Feb 19;108(3):587-96.

Boring BB, Squires TS, Tong T, 1994. Cancer statistics. CA Cancer J. Clin., 44, pp. 7–26

Bowers DC, Gargan L, Kapur P, Reisch JS, Mulne AF, Shapiro KN, Elterman RD, Winick NJ, Margraf LR, 2003. Study of the MIB-1 labeling index as a predictor of tumor progression in pilocytic astrocytomas in children and adolescents. J Clin Oncol. Aug 1; 21(15): 2968-73.

Carvalho da Fonseca AC, Badie B, 2013. Microglia and macrophages in malignant gliomas: recent discoveries and implications for promising therapies. Clin Dev Immunol. 264124.

Cascone T, Heymach JV, 2012. Targeting the angiopoietin/Tie2 pathway: cutting tumor vessels with a double-edged sword? J Clin Oncol. Feb 1; 30(4): 441-4.

Chen L, Zhang Y, Yang J, Hagan JP, Li M, 2013. Vertebrate animal models of glioma: understanding the mechanisms and developing new therapies. Biochim Biophys Acta. Aug; 1836(1): 158-65.

Cullen DK, Simon CM, LaPlaca MC, 2007. Strain rate-dependent induction of reactive astrogliosis and cell death in three-dimensional neuronal-astrocyticco-cultures. Brain Res. Jul 16;1158:103-15.

DeAngelis LM, 2001. Brain tumors. N Engl J Med. Jan 11; 344(2): 114-23.

Domanska UM, Timmer-Bosscha H, Nagengast WB, Oude Munnink TH, Kruizinga RC, Ananias HJ, Kliphuis NM, Huls G, De Vries EG,de Jong IJ, Walenkamp AM, 2012. CXCR4 inhibition with AMD3100 sensitizes prostate cancer to docetaxel chemotherapy. Neoplasia. Aug;14(8):709-18.

Gao JL, Lee EJ, Murphy PM, 1999. Impaired antibacterial host defense in mice lacking the N-formylpeptide receptor. J Exp Med. Feb 15; 189(4): 657-62.

Giese A, Bjerkvig R, Berens ME, Westphal M, 2003. Cost of Migration: Invasion of Malignant Gliomas and Implications for Treatment. JCO April 15, vol. 21 no. 8 1624-1636.

Heusinkveld M, van der Burg SH, 2011. Identification and manipulation of tumor associated macrophages in human cancers. J Transl Med. Dec 16;9:216.

Haas PJ, de Haas CJ, Kleibeuker W, Poppelier MJ, van Kessel KP, Kruijtzer JA, Liskamp RM, van Strijp JA, 2004. N-terminal residues of the chemotaxis inhibitory protein of Staphylococcus aureus are essential for blocking formylated peptide receptor but not C5a receptor. J Immunol. Nov 1;173(9):5704-11.

Heusinkveld M, van der Burg SH, 2011. Identification and manipulation of tumor associated macrophages in human cancers. J Transl Med. Dec 16;9:216.

Houben MP, Aben KK, Teepen JL, Schouten-Van Meeteren AY, Tijssen CC, Van Duijn CM, Coebergh JW, 2006. Stable incidence of childhood and adult glioma in The Netherlands, 1989-2003. Acta Oncol. 45(3): 272-9.

Huang J, Hu J, Bian X, Chen K, Gong W, Dunlop NM, Howard OM, Wang JM, 2007. Transactivation of the epidermal growth factor receptor by formylpeptide receptor exacerbates the malignant behavior of human glioblastoma cells. Cancer Res. Jun 15; 67(12): 5906-13.

Huang J, Chen K, Gong W, Zhou Y, Le Y, Bian X, Wang JM, 2008. Receptor "hijacking" by malignant glioma cells: a tactic for tumor progression. Cancer Lett. Aug 28;267(2):254-61.

Huang J, Chen K, Chen J, Gong W, Dunlop NM, Howard OM, Gao Y, Bian XW, Wang JM, 2010. The G-protein-coupled formylpeptide receptor FPR confers a more invasive phenotype on human glioblastoma cells. Br J Cancer. Mar 16; 102(6): 1052-60.

Jacque CM, Vinner C, Kujas M, Raoul M, Racadot J, Baumann NA, 1978. Determination of glial fibrillary acidic protein (GFAP) in human brain tumors. J Neurol Sci. Jan;35(1):147-55.

Komohara Y, Ohnishi K, Kuratsu J, Takeya M, 2008. Possible involvement of the M2 anti-inflammatory macrophage phenotype in growth of human gliomas. J Pathol. Sep;216(1):15-24.

Kuijlen JM, Mooij JJ, Platteel I, Hoving EW, van der Graaf WT, Span MM, Hollema H, den Dunnen WF, 2006. TRAIL-receptor expression is an independent prognostic factor for survival in patients with a primary glioblastoma multiforme. J Neurooncol. Jun;78(2):161-71.

Le Y, Hu J, Gong W, Shen W, Li B, Dunlop NM, Halverson DO, Blair DG, Wang JM, 2000. Expression of functional formyl peptide receptors by human astrocytoma cell lines. J Neuroimmunol. Nov 1;111(1-2):102-8.

Le Y, Iribarren P, Zhou Y, Gong W, Hu J, Zhang X, Wang JM, 2004. Silencing the formylpeptide receptor FPR by short-interfering RNA. Mol Pharmacol. Oct;66(4):1022-8. Epub Jul 16.

Louis DN, 2006. Molecular pathology of malignant gliomas. Annu Rev Pathol. 1: 97-117.

Louis DN, Ohgaki H, Wiestler OD, Cavenee WK, Burger PC, Jouvet A, Scheithauer BW, Kleihues P, 2007. The 2007 WHO classification of tumours of the central nervous system. Acta Neuropathol. Aug; 114(2): 97-109.

Marasco WA, Phan SH, Krutzsch H, Showell HJ, Feltner DE, Nairn R, Becker EL, Ward PA, 1984. Purification and identification of formyl-methionyl-leucyl-phenylalanine as the major peptide neutrophil chemotactic factor produced by Escherichia coli. J. Biol. Chem., 259, pp. 5430–5439.

Mori T, Kim J, Yamano T, 2005. Epigenetic up-regulation of C-C chemokine receptor 7 and C-X-C chemokine receptor 4 expression in melanoma cells. Cancer Res. **65**: 1800–1807.

Murphy PM, Ozçelik T, Kenney RT, Tiffany HL, McDermott D, Francke U, 1992. A structural homologue of the N-formyl peptide receptor. Characterization and chromosome mapping of a peptide chemoattractant receptor family. J Biol Chem. Apr 15; 267(11): 7637-43.

Murphy PM, 1994. The molecular biology of leukocyte chemoattractant receptors. Annu Rev Immunol. 12: 593-633.

Ohgaki H, Kleihues P, 2005. "Population-based studies on incidence, survival rates, and genetic alterations in astrocytic and oligodendroglial gliomas". J Neuropathol Exp Neurol. 64 (6): 479–89.

Partida-Sánchez S, Cockayne DA, Monard S, Jacobson EL, Oppenheimer N, Garvy B, Kusser K, Goodrich S, Howard M, Harmsen A, Randall TD, Lund FE, 2001. Cyclic ADP-ribose production by CD38 regulates intracellular calcium release, extracellular calcium influx and chemotaxis in neutrophils and is required for bacterial clearance in vivo. Nat Med. Nov; 7(11): 1209-16.

Phillips HS, Kharbanda S, Chen R, Forrest WF, Soriano RH, Wu RD, Misra A, Nigro JM, Colman H, Soroceanu L, 2006. Molecular subclasses of high-grade glioma predict prognosis, delineate a pattern of disease progression, and resemble stages in neurogenesis. Cancer Cell, 9, pp. 157–173

Postma B, Poppelier MJ, van Galen JC, Prossnitz ER, van Strijp JA, de Haas CJ, van Kessel KP, 2004. Chemotaxis inhibitory protein of Staphylococcus aureus binds specifically to the C5a and formylated peptide receptor. J Immunol. Jun 1; 172(11): 6994-7001.

Prossnitz ER, Ye RD, 1997. The N-formyl peptide receptor: a model for the study of chemoattractant receptor structure and function. Pharmacol Ther. 74(1): 73-102.

Rabiet MJ, Huet E, Boulay F, 2005. Human mitochondria-derived N-formylated peptides are novel agonists equally active on FPR and FPRL1, while Listeria monocytogenes-derived peptides preferentially activate FPR. Eur J Immunol. Aug; 35(8): 2486-95.

Showell HJ, Freer RJ, Zigmond SH, Schiffmann E, Aswanikumar S, Corcoran B, Becker EL, 1976. The structure-activity relations of synthetic peptides as chemotactic factors and inducers of lysosomal secretion for neutrophils. J Exp Med. May 1; 143(5): 1154-69.

Song L, Lee C, Schindler C, 2011. Deletion of the murine scavenger receptor CD68. J Lipid Res. Aug;52(8):1542-50.

Stupp R, Hegi ME, Mason WP, van den Bent MJ, Taphoorn MJ, Janzer RC, Ludwin SK, Allgeier A, Fisher B, Belanger K, Hau P, Brandes AA, Gijtenbeek J,Marosi C, Vecht CJ, Mokhtari K, Wesseling P, Villa S, Eisenhauer E, Gorlia T, Weller M, Lacombe D, Cairncross JG, Mirimanoff RO, 2009. Effects of radiotherapy with concomitant and adjuvant temozolomide versus radiotherapy alone on survival in glioblastoma in a randomised phase III study: 5-year analysis of the EORTC-NCIC trial. Lancet Oncol. May;10(5):459-66.

Sullivan R, Graham CH, 2007. Hypoxia-driven selection of the metastatic phenotype. Cancer Metastasis Rev., 26, pp. 319–33
Tiede S, Kloepper JE, Ernst N, 2009. Nestin in human skin: exclusive expression in intramesenchymal skin compartments and regulation by leptin. J Invest Dermatol. 129 (11): 2711–20.

Tohma Y, Gratas C, Biernat W, 1998. PTEN (MMAC1) mutations are frequent in primary glioblastomas (de novo) but not in secondary glioblastomas. J Neuropathol Exp Neurol; 57: 684-689.

Van Meir EG, Hadjipanayis CG, Norden AD, Shu HK, Wen PY, Olson JJ, 2010. Exciting New Advances in Neuro-Oncology: The Avenue to a Cure for Malignant Glioma. CA: A Cancer Journal for Clinicians 60 (3): 166–93.

Verhaak RG, Hoadley KA, Purdom E, Wang V, Qi Y, Wilkerson MD, Miller CR, Ding L, Golub T, Mesirov JP, Alexe G, Lawrence M, O'Kelly M, Tamayo P, Weir BA, Gabriel S, Winckler W, Gupta S, Jakkula L, Feiler HS, Hodgson JG, James CD, Sarkaria JN, Brennan C, Kahn A, Spellman PT, Wilson RK, Speed TP, Gray JW, Meyerson M, Getz G, Perou CM, Hayes DN, 2010. Integrated genomic analysis identifies clinically relevant subtypes of glioblastoma characterized by abnormalities in PDGFRA, IDH1, EGFR, and NF1. Cancer Cell. Jan 19;17(1):98-110.

Wang Y, Jiang T, 2013. Understanding high grade glioma: molecular mechanism, therapy and comprehensive management. Cancer Lett. May 1;331(2):139-46.

Watanabe K, Tachibana O, Sato K, Yonekawa Y, Kleihues P, Ohgaki H, 1996. Overexpression of the EGF receptor and p53 mutations are mutually exclusive in the evolution of primary and secondary glioblastomas. Brain Pathol; 6: 217-223.

Wen PY, Kesari S, 2008. Malignant gliomas in adults. N Engl J Med 359: 492–507

Wilson CB, 1992. Glioblastoma: the past, the present, and the future. Clin. Neurosurg., 38 pp. 32–48.

Yamashita S, 2007. Heat-induced antigen retrieval: mechanisms and application to histochemistry. Prog Histochem Cytochem. 41(3):141-200.

Yang I, Han SJ, Kaur G, Crane C, Parsa AT, 2010. The role of microglia in central nervous system immunity and glioma immunology. Journal of Clinical Neuroscience. 17(1): 6–10.

Yang L, Lin C, Wang L, Guo H, Wang X, 2012. Hypoxia and hypoxia-inducible factors in glioblastoma multiforme progression and therapeutic implications. Exp Cell Res. Nov 15; 318(19): 2417-26.

Yao XH, Ping YF, Chen JH, Chen DL, Xu CP, Zheng J, Wang JM, Bian XW, 2008. Production of angiogenic factors by human glioblastoma cells following activation of the G-protein coupled formylpeptide receptor FPR. J Neurooncol. Jan; 86(1): 47-53.

Ye RD, Cavanagh SL, Quehenberger O, Prossnitz ER, Cochrane CG, 1992. Isolation of a cDNA that encodes a novel granulocyte N-formyl peptide receptor. Biochem Biophys Res Commun. Apr 30; 184(2): 582-9.
Ye RD, Boulay F, Murphey PM, 2009. International Union of Basic and Clinical Pharmacology. LXXIII. Nomenclature for the Formyl Peptide Receptor (FPR) Family. Pharmacol rev. June; 61(2): 119-161.

Zhang JZ, Behrooz A, Ismail-Beigi F, 1999. Regulations of glucose transport by hypoxia. Am J Kidney Dis Jul; 34(1): 189-202.

Zhou Y, Bian X, Le Y, Gong W, Hu J, Zhang X, Wang L, Iribarren P, Salcedo R, Howard OM, Farrar W, Wang JM, 2005. Formylpeptide receptor FPR and the rapid growth of malignant human gliomas. J Natl Cancer Inst. Jun 1; 97(11): 823-35.